

**Trent Stellingwerff, Hanneke Boon, Richard A. M. Jonkers, Joan M. Senden,
Lawrence L. Spriet, René Koopman and Luc J. C. van Loon**
Am J Physiol Endocrinol Metab 292:1715-1723, 2007. First published Feb 13, 2007;
doi:10.1152/ajpendo.00678.2006

You might find this additional information useful...

This article cites 57 articles, 36 of which you can access free at:

<http://ajpendo.physiology.org/cgi/content/full/292/6/E1715#BIBL>

Updated information and services including high-resolution figures, can be found at:

<http://ajpendo.physiology.org/cgi/content/full/292/6/E1715>

Additional material and information about *AJP - Endocrinology and Metabolism* can be found at:

<http://www.the-aps.org/publications/ajpendo>

This information is current as of June 4, 2007 .

Significant intramyocellular lipid use during prolonged cycling in endurance-trained males as assessed by three different methodologies

Trent Stellingwerff,¹ Hanneke Boon,² Richard A. M. Jonkers,¹ Joan M. Senden,¹ Lawrence L. Spriet,³ René Koopman,¹ and Luc J. C. van Loon^{1,2}

Departments of ¹Movement Sciences and ²Human Biology, Nutrition Research Institute Maastricht, Maastricht University, Maastricht, The Netherlands; and ³Department of Human Health and Nutritional Sciences, University of Guelph, Guelph, Canada

Submitted 12 December 2006; accepted in final form 7 February 2007

Stellingwerff T, Boon H, Jonkers RA, Senden JM, Spriet LL, Koopman R, van Loon LJ. Significant intramyocellular lipid use during prolonged cycling in endurance-trained males as assessed by three different methodologies. *Am J Physiol Endocrinol Metab* 292: E1715–E1723, 2007. First published February 13, 2007; doi:10.1152/ajpendo.00678.2006.—Intramyocellular triacylglycerol (IMTG) has been suggested to represent an important substrate source during exercise. In the present study, IMTG utilization during exercise is assessed through the use of various methodologies. In addition, we identified differences in the use of intramyocellular lipids deposited in the immediate subsarcolemmal (SS) area and those stored in the more central region of the fiber. Contemporary stable isotope technology was applied in combination with muscle tissue sampling before and immediately after 3 h of moderate-intensity cycling exercise ($62 \pm 2\%$ $\dot{V}O_{2\max}$) in eight well-trained male cyclists. Continuous infusions with [U - ^{13}C]palmitate and [$6,6$ - 2H_2]glucose were applied to quantify plasma free fatty acid (FFA) and glucose oxidation rates and to estimate whole body IMTG and glycogen use. Both immunohistochemical analyses of oil red O (ORO)-stained muscle cross sections and biochemical triacylglycerol (TG) extraction were performed to assess muscle lipid content. During exercise, plasma FFA, muscle (and/or lipoprotein)-derived TG, plasma glucose, and muscle glycogen oxidation contributed 24 ± 2 , 22 ± 3 , 11 ± 1 , and $43 \pm 3\%$ to total energy expenditure, respectively. In accordance, a significant net decline in muscle lipid content was observed following exercise as assessed by ORO staining ($67 \pm 8\%$) and biochemical TG extraction ($49 \pm 8\%$), and a positive correlation was observed between methods ($r = 0.56$; $P < 0.05$). Lipid depots located in the SS area were utilized to a greater extent than the more centrally located depots. This is the first study to show significant use of IMTG as a substrate source during exercise in healthy males via the concurrent implementation of three major methodologies. In addition, this study shows differences in resting subcellular intramyocellular lipid deposit distribution and in the subsequent net use of these deposits during exercise.

fat metabolism; intramyocellular triacylglycerol; skeletal muscle; cycling; substrate utilization

IT HAS BEEN ESTABLISHED THAT plasma free fatty acid (FFA) oxidation rates account for ~ 50 – 70% of total fat oxidation during moderate-intensity exercise (40, 48). Therefore, other fat sources must contribute substantially to total fat oxidation (47, 53). In accordance, several laboratories using immunofluorescence microscopy on oil red O (ORO)-stained muscle cross sections report a substantial net decline in type I muscle fiber lipid content following exercise in healthy males (10, 28,

51, 52). Nevertheless, there is much controversy regarding the proposed role of intramyocellular triacylglycerol (IMTG) as a substrate source during exercise. Whereas previous studies applying conventional biochemical triacylglycerol (TG) extraction analyses on muscle biopsy samples report significant declines in muscle lipid content following exercise (3, 6, 8, 35, 53), others have failed to observe such changes (26, 39, 43, 55). Furthermore significant declines in IMTG content following exercise have been reported in females but not in males (38, 39, 46). Although biochemical TG extraction analysis provides a direct quantitative assessment of mixed-muscle lipid content, it does not differentiate between fiber-type lipid content and/or intra- and extramyocellular lipid stores. These limitations are likely responsible for the large measurement variability when using this methodology (54). The present study aims to establish whether the IMTG pool represents a viable substrate source during prolonged exercise in healthy, endurance-trained males through the concurrent use of muscle TG extraction analyses, immunofluorescence microscopy on ORO-stained muscle cross sections, and stable isotope tracer methodology.

Besides quantifying muscle fiber type-specific lipid content, the use of immunofluorescence microscopy also allows the assessment of intramyocellular lipid distribution characteristics (49). Our laboratory has recently shown that most of the intramyocellular lipid aggregates are located in the subsarcolemmal (SS) area. Furthermore, lipid droplet density declines exponentially from the periphery toward the central myofibrillar region (49). These findings seem to be in line with earlier reports showing two- to threefold greater mitochondrial density in the SS vs. the intermyofibrillar (IMF) area (7, 12) and the observation that most intramyocellular lipid deposits are in close proximity to mitochondria (5, 17, 18). Furthermore, a preferential proliferation of mitochondria in the SS area has been reported following endurance training (18, 19), and these mitochondria seem to display greater exercise-induced increases in respiratory and oxidative enzyme capacity (4, 12, 30). Therefore, by applying immunofluorescence microscopy on ORO-stained muscle cross sections, we also aimed to assess potential differences in the use of intramyocellular lipid depots located in the immediate SS area vs. the more centrally located lipid depots during exercise. Because of the quantitative and qualitative properties of SS vs. IMF mitochondria, we hypothesized that SS intramyocellular lipid

Address for reprint requests and other correspondence: T. Stellingwerff, Dept. of Movement Science, Maastricht Univ., PO Box 616, 6200 MD, Maastricht, The Netherlands (e-mail: trent.stellingwerff@rdls.nestle.com).

The costs of publication of this article were defrayed in part by the payment of page charges. The article must therefore be hereby marked "advertisement" in accordance with 18 U.S.C. Section 1734 solely to indicate this fact.

would be used to a greater extent during exercise than compared with the more centrally located depots.

METHODS

Subjects. Eight endurance-trained male subjects were selected to participate in this study, and their characteristics are outlined in Table 1. Subjects were informed about the nature and risks of the experimental procedures before their written informed consent was obtained. This study was approved by the local Medical Ethical Committee of the Academic Hospital Maastricht and is part of a larger project investigating the effects of exercise on skeletal muscle substrate use.

Pretesting. Subjects performed a continuous incremental exercise test to exhaustion on a cycle ergometer (Lode, Groningen, The Netherlands) to determine peak pulmonary oxygen uptake ($\dot{V}O_{2\max}$, Oxycon- β ; Mijnhart, Bunnik, The Netherlands) and maximal workload capacity (W_{\max}). After an overnight fast, body composition was assessed using the hydrostatic weighing method, with corrections made for residual lung volume via the helium dilution technique (Volugraph 2000; Mijnhart). Body fat percentage was calculated using Siri's (42) equation.

Diet and activity before testing. All subjects were instructed to maintain normal dietary and physical activity patterns and refrained from heavy physical labor and exercise training for 3 days before the trials. In addition, they filled out a food intake diary for 2 days before the first trial and repeated dietary intake during the subsequent trial. The evening before each trial, all subjects received the same standardized meal [41.2 kJ/kg body wt; containing 72, 11, and 17 energy% carbohydrate (CHO), fat, and protein, respectively]. Dietary analysis showed an average daily energy intake of 12.8 ± 0.7 MJ, of which 57 ± 2 , 28 ± 2 , and 15 ± 1 energy% was derived from CHO, fat and protein, respectively.

Experimental trials. Each subject performed two randomized trials, separated by at least 1 wk: the main experimental trial and an acetate correction trial. Each trial consisted of 60 min of rest, followed by 3 h of cycling at 50% W_{\max} . In the main experimental trial, continuous intravenous infusions with [$U-^{13}C$]palmitate and [6,6- 2H_2]glucose were applied at rest and during exercise with breath, blood, and muscle samples collected at regular intervals. Water was provided to the subjects every 20 min during exercise at a volume of 2.5 ml/kg body wt, resulting in a total water intake of 1.81 ± 0.01 liters. In the second trial, a [1,2- ^{13}C]acetate tracer was infused continuously at rest and during exercise, with only breath samples being collected. The acetate trial was performed for each individual subject to determine the acetate recovery factor to accurately correct [$U-^{13}C$]palmitate oxidation rates for carbon label retention in the bicarbonate pool(s) and by way of isotopic exchange reactions in the tricarboxylic acid

cycle (50). During exercise, acetate label recovery reached a plateau value within 40 min, averaging $86 \pm 1\%$ of the acetate infusion rate throughout the 3-h exercise trial. This plateau value was used to correct the palmitate rate of appearance (R_a) for carbon label retention, as outlined previously (50).

Protocol. After an overnight fast, subjects arrived at the laboratory at 0800 by car or public transportation. After 30 min of supine rest, a percutaneous muscle biopsy was taken from the vastus lateralis muscle at time (t) = 0 min, 1 h before the commencement of exercise (2). A Teflon catheter (Baxter, Utrecht, The Netherlands) was inserted in an antecubital vein of one arm for blood sampling, whereas another catheter was inserted in the antecubital vein of the contralateral arm for isotope infusion. Thereafter, a resting blood sample was taken, and expired breath samples were collected in vacutainer tubes. Subsequently, subjects were administered a single intravenous dose of $NaH^{13}CO_3$ (0.06375 mg/kg), to prime the bicarbonate pool(s), followed by a [6,6- 2H_2]glucose prime (13.5 $\mu\text{mol/kg}$). Thereafter, a continuous infusion of [6,6- 2H_2]glucose (0.3 $\mu\text{mol}\cdot\text{kg}^{-1}\cdot\text{min}^{-1}$) and [$U-^{13}C$]palmitate (0.01 $\mu\text{mol}\cdot\text{kg}^{-1}\cdot\text{min}^{-1}$; or [1,2- ^{13}C]acetate in the acetate recovery trial) was started (t = 0 min) via a calibrated IVAC pump (model 560; IVAC, San Diego, CA) and continued for 4 h. At t = 60 min, an initial water bolus (2.5 ml/kg) was given, and then nine more water boluses were given at t = 80, 100, 120, 140, 160, 180, 200, 220, and 240 min. At t = 60 min, subjects started to exercise on a cycle ergometer at a workload of 50% W_{\max} (202 ± 6 W) for 3 h. Expired $\dot{V}O_2$ and $\dot{V}CO_2$ were measured (Oxycon- β) continuously at rest and for 5 min every 15 min during exercise before sampling of blood and expired breath collection. Immediately after cessation of exercise, a second muscle biopsy was taken (t = 240 min). Breath and blood samples were collected at t = 0, 30, and 60 min (rest) and at t = 80, 100, 120, 140, 160, 180, 200, 220, and 240 min (exercise).

Tracer preparation and infusion. At rest, infusion rates of [$U-^{13}C$]palmitate and [6,6- 2H_2]glucose averaged 7.3 ± 0.3 and 829 ± 6 $\text{nmol}\cdot\text{kg}^{-1}\cdot\text{min}^{-1}$, respectively. At the onset of exercise, [$U-^{13}C$]palmitate infusion rates were doubled (15.0 ± 0.6 $\text{nmol}\cdot\text{kg}^{-1}\cdot\text{min}^{-1}$). In the acetate recovery trial, a corresponding amount of ^{13}C was infused, resulting in an average [1,2- ^{13}C]acetate infusion rate of 61.5 ± 0.5 and 123 ± 1 $\text{nmol}\cdot\text{kg}^{-1}\cdot\text{min}^{-1}$ at rest and during exercise, respectively. Palmitate, glucose, and acetate tracer concentrations in the infusates averaged 1.06 ± 0.02 , 63.5 ± 2.2 , and 4.68 ± 0.03 mmol/l, respectively.

Blood and breath sample analysis. Blood samples (7 ml) were collected in EDTA-containing tubes and centrifuged at 1,000 g for 10 min at 4°C. Aliquots of plasma were frozen immediately in liquid nitrogen and stored at -80°C . Plasma glucose (Uni Kit III; Roche, Basel, Switzerland), lactate (16), FFA (NEFA-C; Wako Chemicals, Neuss, Germany), free glycerol (148270; Roche Diagnostics, Indianapolis, IN), and triglyceride (GPO-trinder 337B; Sigma Diagnostics, St. Louis, MO) concentrations were analyzed with a COBAS semi-automatic analyzer (Roche).

Expired breath samples were analyzed for the ^{13}C -to- ^{12}C ratio by gas chromatography continuous-flow isotope ratio mass spectrometry (GC-IRMS, MAT 252; Finnigan, Bremen, Germany). For determination of plasma palmitate and FFA kinetics, FFA were extracted from plasma, isolated by TLC, and derivatized to their methyl esters. Palmitate concentration was determined on an analytical gas chromatograph with flame ionization detection using heptadecanoic acid as an internal standard and on average comprised $26.0 \pm 0.02\%$ of total FFA. Isotope tracer-to-tracee ratio (TTR) of [$U-^{13}C$]palmitate was determined using GC-combustion IRMS (Finnigan MAT 252). Following derivatization, plasma [6,6- 2H_2]glucose enrichment was determined by electron ionization GC-MS (Finnigan INCOS-XL). Glucose (Uni Kit III; Roche) and acetate (Kit 148261; Boehringer) concentrations in the infusates were determined with the COBAS FARA.

Calculations. Whole body respiratory exchange ratio (RER) was calculated as rates of CO_2 production ($\dot{V}CO_2$) divided by O_2 consump-

Table 1. *Subjects' characteristics*

Age, yr	23 \pm 1
Height, meters	1.82 \pm 0.01
Body mass, kg	70.6 \pm 2.7
BMI, kg/m ²	21.3 \pm 0.6
Body fat percentage, %	9.0 \pm 0.7
Fat-free mass, kg	64.1 \pm 2.1
Basal plasma glucose, mmol/l	5.2 \pm 0.1
Plasma glucose _{120 min} , mmol/l	4.1 \pm 0.4
Basal plasma insulin, mU/l	8.2 \pm 0.8
HbA _{1c} , %	5.2 \pm 0.1
$\dot{V}O_{2\max}$, ml \cdot kg ⁻¹ \cdot min ⁻¹	62 \pm 2
W_{\max} , watts	404 \pm 13

Values are expressed as means \pm SE; n = 8 subjects. W_{\max} , maximum workload capacity. Plasma glucose_{120 min}, plasma glucose concentration 120 min after ingestion of glucose in the oral glucose tolerance test. Body mass index (BMI) is calculated by dividing body mass by ht².

tion ($\dot{V}O_2$). From respiratory measurements, total fat and CHO oxidation rates were calculated using the nonprotein respiratory quotient (34).

$$\text{Fat oxidation rate} = 1.695 \dot{V}O_2 - 1.701 \dot{V}CO_2 \quad (1)$$

$$\text{Carbohydrate oxidation rate} = 4.585 \dot{V}CO_2 - 3.226 \dot{V}O_2 \quad (2)$$

with $\dot{V}O_2$ and $\dot{V}CO_2$ in liter per minute and oxidation rates in gram per minute. Breath and plasma enrichments are expressed as TTR;

$$\text{TTR} = ({}^{13}\text{C}/{}^{12}\text{C})_{\text{sa}} - ({}^{13}\text{C}/{}^{12}\text{C})_{\text{bk}} \quad (3)$$

in which sa indicates sample and bk indicates background value. Palmitate and glucose R_a and rate of disappearance (R_d) were calculated using the single-pool non-steady-state Steele equations (45) adapted for stable isotope methodology as described elsewhere (57). As such, plasma palmitate and glucose R_d were calculated by correcting the R_a for the time-dependent changes in plasma metabolite concentration.

$$R_a = \frac{F - V[(C_2 + C_1)/2][(E_2 - E_1)/(t_2 - t_1)]}{(E_2 + E_1)/2} \quad (4)$$

$$R_d = R_a - V \times \left(\frac{C_2 - C_1}{t_2 - t_1} \right) \quad (5)$$

where F is the infusion rate ($\mu\text{mol} \cdot \text{kg}^{-1} \cdot \text{min}^{-1}$); V is the distribution volume for palmitate or glucose (40 and 160 ml/kg, respectively); C_1 and C_2 are the palmitate or glucose concentrations (mmol/l) at time 1 (t_1) and 2 (t_2), respectively; and E_2 and E_1 are the plasma palmitate or glucose enrichments (TTR) at time 1 and 2, respectively. ${}^{13}\text{CO}_2$ production ($\text{Pr}^{13}\text{CO}_2$; mol/min) from the infused palmitate tracer was calculated as:

$$\text{Pr}^{13}\text{CO}_2 = (\text{TTR}_{\text{CO}_2} \times \dot{V}CO_2)/(k \times \text{Ar}) \quad (6)$$

where TTR_{CO_2} is the breath ${}^{13}\text{C}$ -to- ${}^{12}\text{C}$ ratio at a given time point; $\dot{V}CO_2$ is the carbon dioxide production (l/min); k is the volume of 1 mol of CO_2 (22.4 l/mol); and Ar is the fractional ${}^{13}\text{C}$ label recovery in breath CO_2 , observed after the infusion of labeled acetate (41) and calculated as:

$$\text{Ar} = [(\text{TTR}_{\text{CO}_2} \times \dot{V}CO_2)/(k \times 2F)] \quad (7)$$

where F is infusion rate of [1,2- ${}^{13}\text{C}$]acetate (mol/min). Plasma palmitate oxidation (R_{ox} ; mol/min) can subsequently be calculated as:

$$R_{\text{ox}} \text{ palmitate} = R_d \text{ palmitate} (\text{Pr}^{13}\text{CO}_2/F \times 16) \quad (8)$$

where R_d palmitate is the rate of palmitate disappearance (mol/min); F is the palmitate infusion rate (mol/min); and 16 is the number of carbon atoms in palmitate. Total plasma FFA oxidation was calculated by dividing palmitate oxidation rates by the fractional contribution of plasma palmitate to total plasma FFA concentration. Muscle-derived TG use was estimated by subtracting plasma FFA oxidation from total fat oxidation. However, it should be noted that the indirect stable isotope methodology does not differentiate between muscle- and lipoprotein-derived TG use. However, the contribution of lipoprotein-derived TG oxidation to total energy expenditure is assumed to be of relative minor quantitative importance, especially in an overnight-fasted state (47). In a previous study, where we applied both a [${}^{13}\text{C}$]- and [${}^{6,6}\text{-}^2\text{H}_2$]glucose tracer (23) during moderate-intensity exercise, it was shown that the percentage of plasma glucose R_d that was oxidized varied between 96 and 100%. Therefore, plasma glucose oxidation rate during exercise was calculated as:

$$R_{\text{ox}} \text{ plasma glucose} = R_d \text{ plasma glucose (during exercise)} \quad (9)$$

Therefore, muscle glycogen oxidation was calculated by subtracting plasma glucose oxidation from total CHO oxidation.

Immunohistochemistry. Muscle samples were freed from any visible nonmuscle material and rapidly frozen in liquid nitrogen. About

15 mg of each muscle sample was frozen in liquid nitrogen-cooled isopentane and embedded in Tissue-Tek (Sakura Finetek, Zoeterwoude, The Netherlands). Multiple serial sections (5 μm) of both muscle biopsy samples from each subject were thaw mounted together on uncoated, precleaned glass slides and stained with ORO (28) to compare intramyocellular lipid content. To determine muscle fiber typing (type I vs. type II), we performed a myosin ATPase stain (32). As described previously, these epifluorescence and bright-field microscopy techniques represent semiquantitative methods that can be used to compare fiber type-specific IMTG contents (49, 51, 52). Fiber type-specific IMTG content was expressed as the fraction of the measured area that was stained with ORO. Mixed-muscle lipid content, lipid droplet size, and lipid droplet density were determined by calculating the average value in the type I and type II muscle fibers, with a correction for the relative area occupied by each fiber type within each field of view of each muscle cross section, within each individual subject. For the average pre- to post-IMTG quantification, the ORO epifluorescence signal was recorded for each muscle fiber, resulting in a total of 76 ± 6 muscle fibers analyzed for each muscle cross section (46 ± 5 type I, 27 ± 2 type II).

As described in more detail previously (49), the captured IMTG images were processed and analyzed for subcellular localization of IMTG in different consecutive 2- μm layers using Lucia 4.81 software (Nikon, Düsseldorf, Germany). In short, an intensity threshold representing minimal- and maximal-intensity values corresponding to lipid droplets was manually set and uniformly used for all images, and then total measured area and then number of objects emitting an ORO epifluorescence signal were recorded. We recorded the location of lipid droplets and resultant area fraction within nine successive bands of 2 μm in width from the SS toward the central region of each muscle fiber cross section. For the intramyocellular localization of lipid content, 139 and 149 type I muscle fibers were assessed from pre- and postexercise muscle biopsies, respectively (an average of 18 ± 4 /muscle sample).

Biochemical extraction of IMTG. IMTG content was determined from a 5- to 10-mg aliquot (~ 25 – 40 mg wet wt) of powdered freeze-dried muscle (15). Briefly, the IMTG was extracted, as originally described by Folch et al. (14), and the chloroform phase was evaporated. After reconstitution, the phospholipids were removed with the addition of silicic acid. The IMTG was saponified, and the free glycerol was assayed fluorometrically in duplicates (1).

Statistics. All data are expressed as means \pm SE. To compare tracer kinetics, substrate utilization rates, IMTG contents, and/or plasma metabolite concentrations over time, a repeated-measures ANOVA was applied. When a significant F ratio was obtained, post hoc analysis was completed using a Student-Newman-Keul's test. To compare pre- to postutilization of lipid within each subsequent layer, a two-way repeated-measures ANOVA was used, using time and layer as factors. For non-time-dependent variables, a Student's *t*-test for paired observations was used. Pearson's linear regression analysis was used to determine any potential linear relationship between variables. Statistical significance was accepted at $P < 0.05$.

RESULTS

Resting energy expenditure was 5.3 ± 0.2 kJ/min and increased >10 -fold after the onset of exercise to 57 ± 2 kJ/min. The applied 50% W_{max} workload resulted in subjects cycling at 202 ± 6 watts, corresponding with a relative workload of $62 \pm 2\%$ $\dot{V}O_{2 \text{ max}}$ (Table 1).

Isotope tracer kinetics. Because plasma FFA and glucose concentrations varied over time in both trials (Fig. 1, A and B), non-steady-state Steele equations were applied to calculate tracer kinetics (45). Both plasma glucose R_a and R_d continually increased over time during exercise ($P < 0.001$). Plasma glucose R_d represented $96 \pm 1\%$ of plasma glucose R_a

throughout the 3-h exercise trial. Plasma palmitate R_a , R_d , and R_{ox} increased continuously during exercise ($P < 0.001$), and $96 \pm 2\%$ of palmitate R_a was oxidized during exercise.

Whole body substrate source utilization. Collected respiratory measures at rest and during exercise are outlined in Table 2. On average, throughout the exercise period, $\dot{V}O_2$ and $\dot{V}CO_2$ were 2.71 ± 0.08 and 2.32 ± 0.07 l/min, respectively. This resulted in an average respiratory exchange ratio of 0.86 ± 0.01 , which translates into 54 ± 3 and $46 \pm 3\%$ of whole body energy expenditure derived from total CHO and fat oxidation, respectively (34). During exercise, total fat oxidation rates signifi-

cantly increased over time, with a concomitant decline in total CHO oxidation rates ($P < 0.001$). The increase in total fat oxidation rate throughout exercise was entirely attributed to a rise in plasma FFA R_a , R_d , and R_{ox} ($P < 0.001$; Table 2), since the oxidation rate of muscle- and/or lipoprotein-derived TG declined over time ($P < 0.001$).

Calculated over the entire 3-h exercise period, total fat oxidation rates averaged 0.64 ± 0.04 g/min, with plasma FFA oxidation contributing $24 \pm 2\%$ of total energy expenditure and the use of other fat sources contributing $22 \pm 2\%$ (Fig. 2). Conversely, the decrease in CHO oxidation rates during exer-

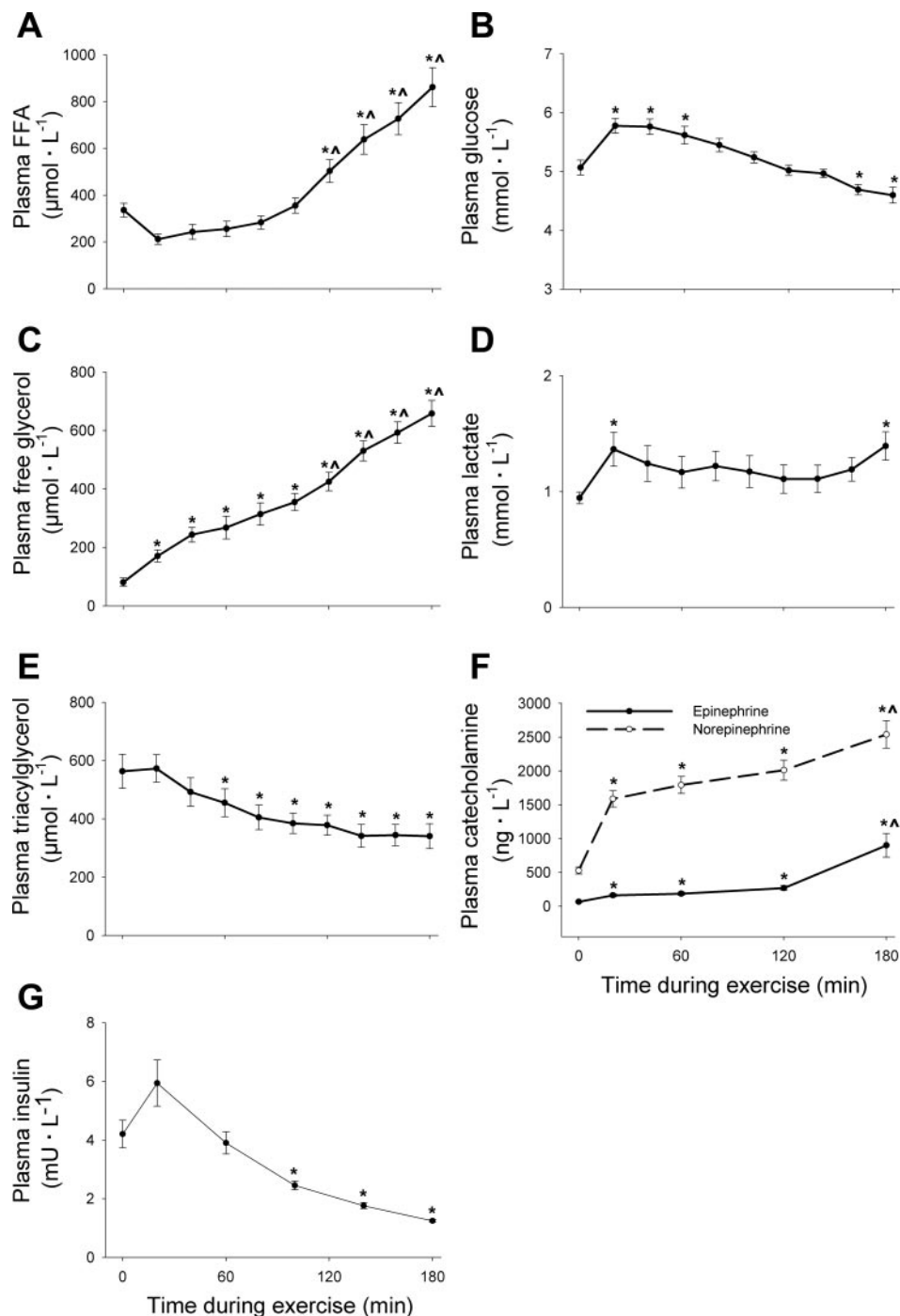


Fig. 1. Plasma metabolite concentrations (A-G) during 3 h of exercise at 50% maximum workload capacity (W_{max}). Values are means \pm SE; $n = 8$ experiments. $P < 0.05$, significantly different from 0 min (*) and significantly different than previous time point (^). FFA, free fatty acid.

Table 2. Tracer kinetics and respiratory measures during rest and exercise

	Rest	3 h Exercise Average
Glucose		
R _a , μmol·kg ⁻¹ ·min ⁻¹	14.67±0.74	30.40±1.89*
R _d , μmol·kg ⁻¹ ·min ⁻¹	15.44±0.78	31.59±1.89*
Palmitate		
R _a , μmol·kg ⁻¹ ·min ⁻¹	1.75±0.09	4.49±0.26*
R _d , μmol·kg ⁻¹ ·min ⁻¹	1.72±0.08	4.44±0.26*
R _{ox} , μmol·kg ⁻¹ ·min ⁻¹	0.64±0.03	4.32±0.22*
R _{a ox} , %	36.8±1.4	95.9±2.1*
Ac recovery, %	14.1±0.1	86.1±0.1*
Respiratory measures		
V _{O₂} , ml	253±9	2,708±81*
V _{CO₂} , ml	209±8	2,321±69*
RER	0.828±0.008	0.858±0.007*

Values are means ± SE; *n* = 8 subjects. R_a, rate of appearance; R_d, rate of disappearance; R_{ox}, rate of oxidation; R_{a ox}, percentage of R_a oxidized (%); Ac recovery, fraction of [1,2-¹³C] acetate label recovery in expired CO₂; RER, respiratory exchange ratio. *Significantly different from rest (*P* < 0.05).

cise was attributed to a decline in muscle glycogen use (*P* < 0.001), since plasma glucose oxidation rates increased progressively (*P* < 0.001). Total CHO oxidation rates averaged 1.91 ± 0.10 g/min, with muscle glycogen and plasma glucose use contributing 43 ± 3 and 11 ± 1% to total energy expenditure, respectively.

Plasma metabolite and hormone concentrations. Plasma FFA, TG, glycerol, glucose, lactate, insulin, and catecholamine concentrations over time during exercise are shown in Fig. 1. Following the onset of exercise, both plasma FFA and glycerol concentrations continually increased from resting values, reaching peak values after cessation of exercise (Fig. 1, A and C). Conversely, plasma TG concentrations continually declined throughout the exercise period (Fig. 1E). During the 1st h of exercise, plasma glucose concentrations increased (*P* < 0.05) above resting concentrations, after which they gradually declined (Fig. 2B). Plasma insulin concentrations declined throughout the exercise period (Fig. 1G) and were significantly lower compared with basal levels during the last 90 min of exercise (*P* < 0.05). Within the first 20 min of exercise, plasma lactate concentrations increased above resting levels (*P* < 0.05; Fig. 1D), after which concentrations returned to preexercise concentrations. Near the latter stages of exercise, plasma lactate levels increased significantly (*P* < 0.05). Plasma norepinephrine concentrations increased threefold within the first 20 min of exercise and continued to rise throughout exercise (Fig. 1F). Plasma epinephrine levels increased gradually during the first 2 h of exercise. Both plasma norepinephrine and epinephrine levels increased substantially within the last hour of exercise (*P* < 0.001; Fig. 1F).

Skeletal muscle lipid content, distribution, and utilization. Figure 3 illustrates representative images of muscle cross sections obtained before (left) and immediately after (right) exercise, as stained for intramyocellular lipid content. Preexercise muscle lipid content was 3.2-fold greater in the type I vs. type II muscle fibers [0.068 ± 0.010 vs. 0.021 ± 0.004 arbitrary units (AU), respectively; *P* < 0.001]. Type I muscle fiber lipid content was 76 ± 7% lower in muscle tissue obtained after exercise (*P* < 0.0001). Type II muscle fiber lipid content tended to be lower in muscle samples collected after

cessation of exercise compared with resting values (*P* = 0.061). After correcting for muscle fiber type composition, mixed-muscle IMTG content, as assessed by immunohistochemical analyses of ORO-stained muscle cross section, was reduced by 67 ± 8% following exercise (Fig. 4A). In accordance, we observed a 49 ± 8% net decline in mixed-muscle IMTG content as quantified by way of biochemical TG extraction analyses performed on the same muscle biopsy samples taken before (24.6 ± 3.1) and after (11.4 ± 1.8 mmol/kg dry wt) exercise (Fig. 4B).

IMTG distribution is presented in Fig. 5 as lipid content, expressed as area fraction lipid stained and corrected for the measured area, in nine successive 2-μm layers from the immediate SS area toward the more central region of the fiber. Resting muscle biopsies showed a decline in intramyocellular lipid droplet content from the SS area toward the center of the fiber (*P* < 0.001; Fig. 5A). On average, 31 ± 3% of the lipid present in the cell is situated within the first two SS layers (0–4 μm), representing only 22 ± 1% of the total cell area. Following exercise, a significant decline in lipid content was observed in all 2-μm layers (*P* < 0.01). However, a significantly greater net decline in intramyocellular lipid content was observed in the SS area (Fig. 5B), with the more central region of each fiber showing an attenuated decline in lipid content when compared with the 0- to 4-μm layers (*P* < 0.01).

Strong positive correlations were observed between resting IMTG content and the subsequent net decline in IMTG content following exercise, as assessed by biochemical TG extraction analyses (*r* = 0.85; *P* < 0.01; Fig. 6A), immunohistochemical analyses of ORO-stained muscle cross sections (*r* = 0.85; *P* < 0.001; Fig. 6B), as well as by examining the intramyocellular lipid content in the successive layers in type I muscle fibers in each individual subject (*r* = 0.93; *P* < 0.001; Fig. 6C).

Correlations between muscle lipid content assessment methods. Mixed-muscle intramyocellular lipid content as quantified by immunohistochemical analyses of ORO-stained muscle cross sections showed a positive correlation with mixed-muscle lipid content as assessed by the biochemical TG extraction analyses (*r* = 0.56; *P* < 0.05). Whole body muscle (and/or lipoprotein)-derived TG oxidation rates during exercise (as assessed by stable isotope methodology) did not correlate with the net decline in mixed-muscle lipid content as quantified by either immunohistochemical staining (*r* = 0.46; *P* = 0.25) or

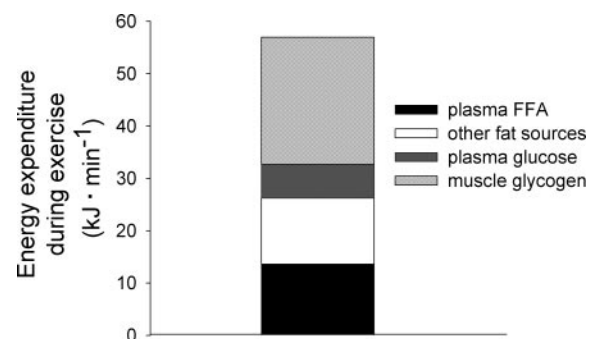
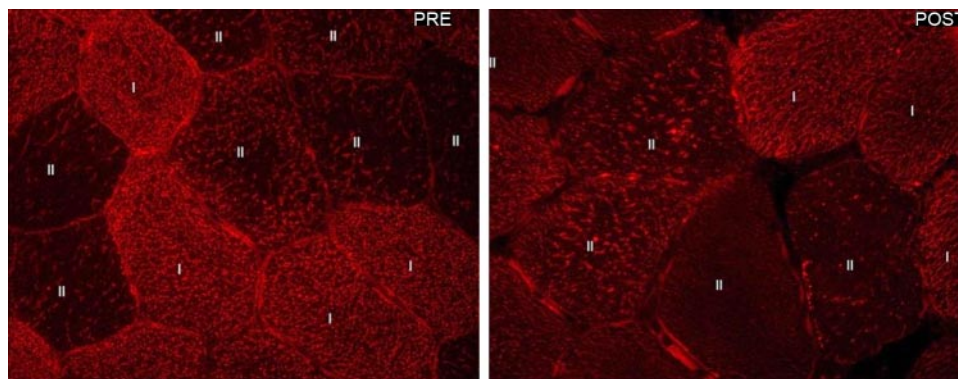


Fig. 2. Average substrate source utilization rates (kJ/min) during 3 h of exercise at 50% W_{max}. Plasma FFA and glucose oxidation rates increased significantly over time, whereas the utilization rate of other muscle (and/or lipoprotein)-derived triacylglycerol (TG) and muscle glycogen declined over time (*P* < 0.001).

Fig. 3. Images ($\times 240$ magnification) of representative cross sections of vastus lateralis muscle obtained before (*left*) and immediately after (*right*) exercise with sections stained for intramyocellular lipid content. The muscle fibers are labeled as type I and type II. Differentiation between type I and II fibres was based on standard ATPase staining.



biochemical TG extraction analyses of muscle lipid content in biopsy samples taken from the vastus lateralis before and after exercise ($r = 0.15$; $P = 0.73$).

DISCUSSION

This is the first study to apply three different methodologies to establish that skeletal muscle lipid stores represent an important substrate source during prolonged exercise in endur-

ance-trained males. In agreement with the large contribution of muscle (and/or lipoprotein)-derived TG use to energy expenditure during exercise, we observed a substantial net decline in skeletal muscle lipid content following prolonged exercise as assessed by using immunofluorescence microscopy on ORO-stained muscle cross sections and by biochemical TG extraction analyses. Furthermore, most intramyocellular lipid depos-

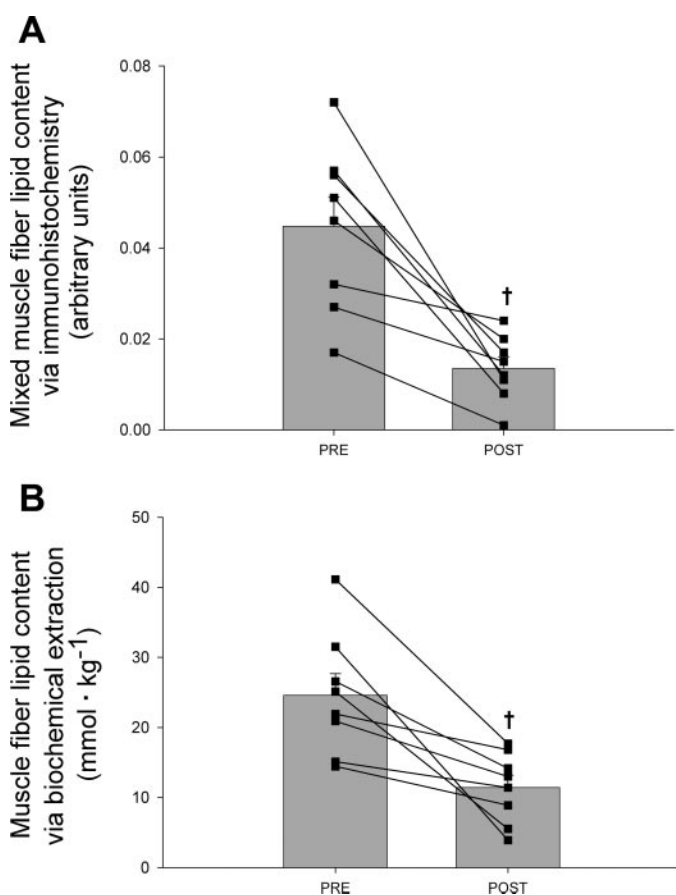


Fig. 4. Intramyocellular lipid content before and after 3 h of exercise at 50% W_{max} as assessed via immunohistochemical analyses of oil red O-stained muscle cross sections (percentage of area lipid stained was assessed per fiber type and calculated for total mixed muscle by correcting for fiber type composition and fiber area; *A*) and biochemical TG extraction analyses ($mmol/kg$ dry wt; *B*). Values are means \pm SE; $n = 8$. Line plots show individual responses ($n = 8$). †Significantly lower than preexercise, resting values ($P < 0.01$).

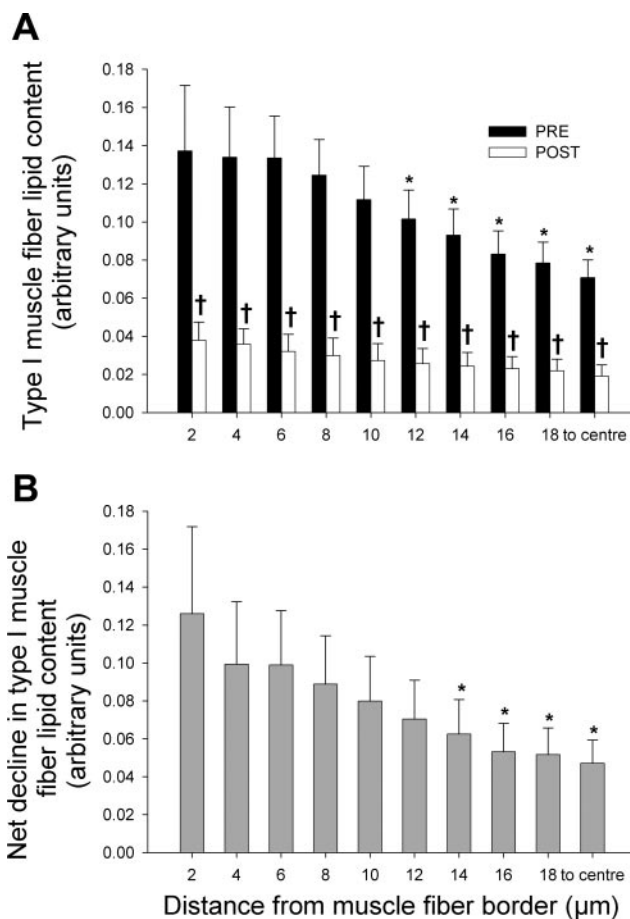


Fig. 5. Type I muscle fiber lipid distribution presented as intramyocellular lipid content (expressed as area fraction lipid stained) in 9 successive 2- μm bands from the immediate subsarcolemmal area toward the more central region of the muscle fiber. *A*: myocellular lipid content before and immediately after 3 h of moderate-intensity exercise. *B*: net changes in myocellular lipid content following 3 h of moderate-intensity exercise. Values are means \pm SE; $n = 8$. $P < 0.001$, significantly less lipid compared with the subsarcolemmal area (0- to 4- μm bands: $P < 0.001$; *) and significantly lower than preexercise values (†).

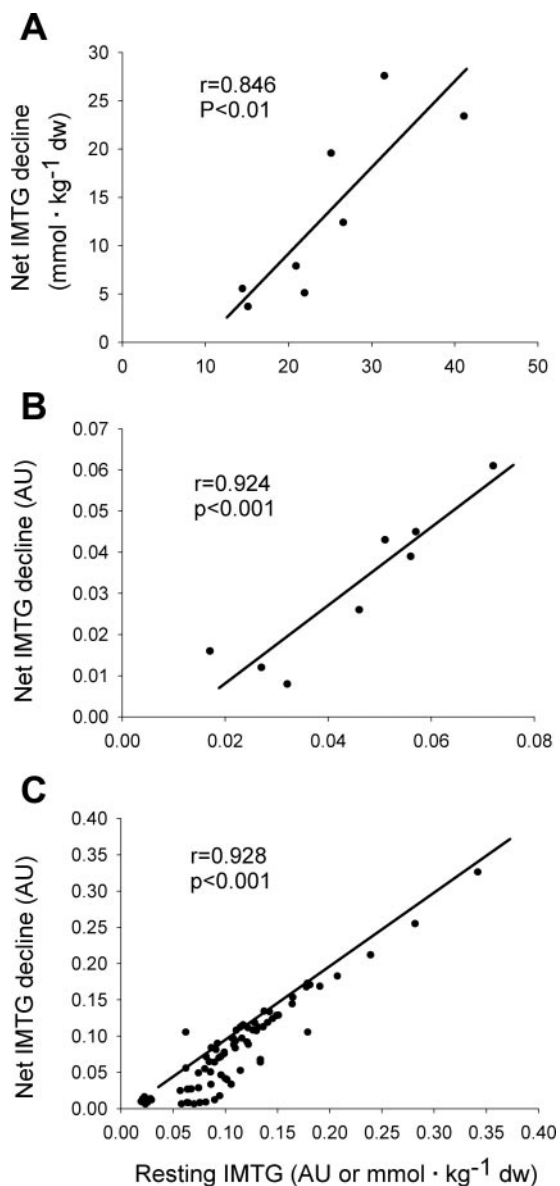


Fig. 6. Correlations between preexercise resting muscle lipid content and the subsequent net decline in muscle lipid content following 3 h of moderate-intensity exercise as assessed via mixed-muscle biochemical TG extraction analyses (mmol/kg dry wt; A), immunohistochemical oil red O-stained muscle cross sections [arbitrary units (AU), percentage of area lipid stained; B], and intramyocellular lipid content assessment of individual 2- μ m bands (9 successive bands) by immunohistochemical analyses (AU, percentage of area lipid stained; C). IMTG, intramyocellular triacylglycerol.

its are stored in the SS area of type I muscle fibers and are used to a greater extent during exercise compared with the more centrally located lipid deposits.

IMTG use during exercise. Even though many previous studies have reported a significant contribution of IMTG as a fuel source during endurance exercise (3, 8, 35, 53), others have failed to support such findings (26, 39, 43, 55). Furthermore, several gender comparison studies have reported a net decline in IMTG content following exercise in females as opposed to males (38, 39, 46). Conversely, Krssak et al. (31) reported a net decline in IMTG in males and females as measured by ¹H-magnetic resonance spectroscopy (MRS). The

apparent inconsistency is likely attributed to the methodological limitations associated with biochemical TG extraction analyses (for reviews, see Refs. 47 and 54). More recent studies assessing IMTG use by applying either stable isotope tracer methodology (9, 40, 48, 51), MRS (5, 11, 31, 52, 58), electron microscopy (25, 44), and/or immunofluorescence microscopy on ORO-stained muscle cross sections (28, 51, 52) have all reported a significant contribution of the IMTG pool as a substrate source during exercise in healthy men. In the present study, stable isotope methodology showed a $22 \pm 2\%$ contribution of muscle (and/or lipoprotein)-derived TG use to whole body energy expenditure during exercise (Fig. 2). This finding was associated with a substantial net decline in IMTG content as assessed by TG extraction analyses ($49 \pm 8\%$ reduction; Fig. 4A) and immunofluorescence microscopy ($67 \pm 8\%$ reduction; Fig. 4B). The advantage of the biochemical TG extraction analysis is that it provides an absolute measure of muscle TG content (54). In this study, skeletal muscle tissue lipid content was shown to decline from 24.6 ± 3.1 to 11.4 ± 1.8 mmol/kg dry wt following the 3 h of exercise. Assuming an active muscle mass between 10 and 15 kg, this would translate into 30–45 g of skeletal muscle lipid being oxidized, representing ~ 30 –45% of total fat oxidation during exercise. However, TG extraction analysis does not permit differentiation between type I and II muscle fiber lipid content. Immunofluorescence microscopy on ORO-stained muscle cross sections can be used to assess fiber type-specific lipid content (Fig. 3). In accordance with previous reports (13, 21, 27, 51, 52), we observed a 3.2-fold greater IMTG content in the type I vs. type II muscle fibers. Furthermore, it was evident that IMTG use predominantly occurred in the type I muscle fibers as opposed to the type II fibers, with a 76 ± 7 and $32 \pm 20\%$ reduction in lipid content, respectively, following exercise.

In the present study, we observed a significant correlation between IMTG content as quantified by biochemical TG extraction analyses and immunofluorescence microscopy on ORO-stained muscle cross sections ($r = 0.559$; $P < 0.05$). Howald et al. (20) previously showed in untrained subjects that resting muscle TG content as assessed by biochemical TG extraction analyses does not correlate well with IMTG assessments via electron microscopy or ¹H-MRS-based analyses. However, it should be noted that most of the problems associated with the biochemical TG extraction method are generally encountered in muscle tissue obtained from untrained sedentary, overweight, and/or obese subjects because of extramyocellular lipid contamination (54, 55), and the present study used endurance-trained subjects. We did not observe significant correlations between whole body muscle (and/or lipoprotein)-derived TG oxidation rates during exercise with the net decline in IMTG content as assessed either by ORO staining ($r = 0.46$; $P = 0.25$) or TG extraction analyses ($r = 0.15$; $P = 0.73$). The lack of such a correlation has been reported previously (51) and is explained by the fact that the net decline in IMTG content in the muscle tissue sample taken from the vastus lateralis is unlikely representative to whole body TG oxidation during exercise. In accordance, substantial differences have been reported in IMTG content and muscle oxidative capacity between various muscle groups (22).

Localization and utilization of intramyocellular lipid deposits. A total of $31 \pm 3\%$ of the intramyocellular lipid deposits was shown to be located within the immediate SS area (here defined

as the surface layer within the first 0–4 μm of the sarcolemma), representing only $22 \pm 1\%$ of the total cell area. These findings are in accordance with previous work examining myocellular lipid distribution patterns (33, 49). We extend on these findings by assessing the subsequent distributional decline in intramyocellular lipid deposits following exercise. We observed a greater decline in intramyocellular lipid located in the immediate SS area compared with the more centrally located deposits (Fig. 5, A and B). These findings are likely associated with the distribution of the intramyocellular mitochondria and the unique metabolic properties of the SS and IMF mitochondria. Boesch et al. (5) and Hoppeler et al. (17, 18) have consistently shown that the majority of intramyocellular lipid deposits are located in close proximity to muscle mitochondria and that there is a preferential proliferation of the SS mitochondria in the endurance-trained state (17–19). In addition, the SS mitochondria display greater volume density, greater exercise-induced increases in respiratory and oxidative enzyme capacity, and enhanced fat oxidative capacity compared with the IMF mitochondria (4, 7, 12, 29, 30). In accordance to our hypothesis, we reported a greater net decline in the intramyocellular lipid stores located in the immediate SS area following exercise compared with the more centrally located lipid deposits (Fig. 5B). As such, we conclude that SS intramyocellular lipid deposits serve a unique and important role as a substrate source during exercise. It has been suggested that SS, as opposed to IMF mitochondria, are of greater metabolic significance to fat oxidation, glucose transport, and the optimal functioning of the insulin-signaling cascade (29, 37). Thus it could be of interest to investigate the impact of exercise, diet, and/or pharmaceutical intervention on intramyocellular lipid deposit location and utilization in subjects with chronic metabolic diseases.

Net decline in IMTG content strongly correlates with pre-exercise IMTG storage. We observed strong positive correlations between preexercise IMTG content and the subsequent net decline following exercise (1) as assessed by TG extraction analyses (Fig. 6A), (2) as assessed by immunofluorescence microscopy (Fig. 6B), and (3) by examining intramyocellular lipid content in successive 2- μm layers within each myofiber (Fig. 6C). These findings confirm previous observations and imply that the level of preexercise IMTG storage determines its subsequent oxidation rate during exercise (24, 38, 46, 51, 56, 58, 59). Based on recent findings by Prats et al. (36), it could be speculated that this proposed relationship is driven by an enhanced enzyme-to-substrate interaction. A greater resting intramyocellular lipid droplet density might improve translocation efficiency of hormone-sensitive lipase to the lipid stores, resulting in greater IMTG mobilization and/or oxidation.

In conclusion, through the concurrent use of immunohistochemical analyses of ORO-stained muscle cross sections, biochemical TG extraction analyses, and contemporary whole body isotope tracer methodology, this study firmly establishes that intramyocellular lipid represents a viable substrate source during prolonged moderate-intensity exercise in healthy, endurance-trained males. Furthermore, intramyocellular lipid use during exercise is shown to be closely correlated to preexercise muscle lipid content. Most intramyocellular lipid deposits are located within the SS area of the type I muscle fiber and are utilized to a greater extent during exercise compared with the more centrally located lipid deposits.

ACKNOWLEDGMENTS

We gratefully acknowledge the expert analytical assistance of Annemie Gijsen, Hanne Vanderey, Antoine Zorence, and Jos Stegen, as well as the enthusiastic support of all the subjects who participated in these trials.

GRANTS

T. Stellingwerff was supported by an individual postdoctorate fellowship from Natural Science and Engineering Research Council of Canada.

REFERENCES

1. Bergmeyer HU. *Methods in Enzymatic Analysis*. New York: Academic, 1974.
2. Bergstrom J. Percutaneous needle biopsy of skeletal muscle in physiological and clinical research. *Scand J Clin Lab Invest* 35: 609–616, 1975.
3. Bergstrom J, Hultman E, Saltin B. Muscle glycogen consumption during cross-country skiing (the Vasa ski race). *Int Z Angew Physiol* 31: 71–75, 1973.
4. Bizeau ME, Willis WT, Hazel JR. Differential responses to endurance training in subsarcolemmal and intermyofibrillar mitochondria. *J Appl Physiol* 85: 1279–1284, 1998.
5. Boesch C, Slotboom J, Hoppeler H, Kreis R. In vivo determination of intra-myocellular lipids in human muscle by means of localized ¹H-MR spectroscopy. *Magn Reson Med* 37: 484–493, 1997.
6. Carlson LA, Ekelund LG, Froberg SO. Concentration of triglycerides, phospholipids and glycogen in skeletal muscle and of free fatty acids and beta-hydroxybutyric acid in blood in man in response to exercise. *Eur J Clin Invest* 1: 248–254, 1971.
7. Cogswell AM, Stevens RJ, Hood DA. Properties of skeletal muscle mitochondria isolated from subsarcolemmal and intermyofibrillar regions. *Am J Physiol Cell Physiol* 264: C383–C389, 1993.
8. Costill DL, Gollnick PD, Jansson ED, Saltin B, Stein EM. Glycogen depletion pattern in human muscle fibres during distance running. *Acta Physiol Scand* 89: 374–383, 1973.
9. Coyle EF, Jeukendrup AE, Wagenmakers AJ, Saris WH. Fatty acid oxidation is directly regulated by carbohydrate metabolism during exercise. *Am J Physiol Endocrinol Metab* 273: E268–E275, 1997.
10. De Bock K, Richter EA, Russell AP, Eijnde BO, Derave W, Ramaekers M, Koninckx E, Leger B, Verhaeghe J, Hespel P. Exercise in the fasted state facilitates fibre type-specific intramyocellular lipid breakdown and stimulates glycogen resynthesis in humans. *J Physiol* 564: 649–660, 2005.
11. Decombaz J, Schmitt B, Ith M, Decarli B, Diem P, Kreis R, Hoppeler H, Boesch C. Postexercise fat intake repletes intramyocellular lipids but no faster in trained than in sedentary subjects. *Am J Physiol Regul Integr Comp Physiol* 281: R760–R769, 2001.
12. Elander A, Sjostrom M, Lundgren F, Schersten T, Bylund-Fellenius AC. Biochemical and morphometric properties of mitochondrial populations in human muscle fibres. *Clin Sci (Lond)* 69: 153–164, 1985.
13. Essen B, Jansson E, Henriksson J, Taylor AW, Saltin B. Metabolic characteristics of fibre types in human skeletal muscle. *Acta Physiol Scand* 95: 153–165, 1975.
14. Folch J, Lees M, Sloane Stanley GH. A simple method for the isolation and purification of total lipides from animal tissues. *J Biol Chem* 226: 497–509, 1957.
15. Frayn KN, Maycock PF. Skeletal muscle triacylglycerol in the rat: methods for sampling and measurement, and studies of biological variability. *J Lipid Res* 21: 139–144, 1980.
16. Gutmann I, Wahlefeld AW. L-(+)-Lactate determination with lactate dehydrogenase and NAD. In: *Methods in Enzymatic Analysis* (2nd ed.), edited by Bergmeyer HU. New York: Academic, 1974, p. 1464–1468.
17. Hoppeler H, Billeter R, Horvath PJ, Leddy JJ, Pendergast DR. Muscle structure with low- and high-fat diets in well-trained male runners. *Int J Sports Med* 20: 522–526, 1999.
18. Hoppeler H, Howald H, Conley K, Lindstedt SL, Claassen H, Vock P, Weibel ER. Endurance training in humans: aerobic capacity and structure of skeletal muscle. *J Appl Physiol* 59: 320–327, 1985.
19. Hoppeler H, Luthi P, Claassen H, Weibel ER, Howald H. The ultrastructure of the normal human skeletal muscle. A morphometric analysis on untrained men, women and well-trained orienteers. *Pflugers Arch* 344: 217–232, 1973.
20. Howald H, Boesch C, Kreis R, Matter S, Billeter R, Essen-Gustavsson B, Hoppeler H. Content of intramyocellular lipids derived by electron microscopy, biochemical assays, and (1)H-MR spectroscopy. *J Appl Physiol* 92: 2264–2272, 2002.

21. Howald H, Hoppeler H, Claassen H, Mathieu O, Straub R. Influences of endurance training on the ultrastructural composition of the different muscle fiber types in humans. *Pflügers Arch* 403: 369–376, 1985.
22. Hwang JH, Pan JW, Heydari S, Hetherington HP, Stein DT. Regional differences in intramyocellular lipids in humans observed by in vivo ¹H-MR spectroscopic imaging. *J Appl Physiol* 90: 1267–1274, 2001.
23. Jeukendrup AE, Raben A, Gijsen A, Stegen JH, Brouns F, Saris WH, Wagenmakers AJ. Glucose kinetics during prolonged exercise in highly trained human subjects: effect of glucose ingestion. *J Physiol* 515: 579–589, 1999.
24. Johnson NA, Stannard SR, Mehalski K, Trenell MI, Sachinwalla T, Thompson CH, Thompson MW. Intramyocellular triacylglycerol in prolonged cycling with high- and low-carbohydrate availability. *J Appl Physiol* 94: 1365–1372, 2003.
25. Kayar SR, Hoppeler H, Howald H, Claassen H, Oberholzer F. Acute effects of endurance exercise on mitochondrial distribution and skeletal muscle morphology. *Eur J Appl Physiol Occup Physiol* 54: 578–584, 1986.
26. Kiens B, Richter EA. Utilization of skeletal muscle triacylglycerol during postexercise recovery in humans. *Am J Physiol Endocrinol Metab* 275: E332–E337, 1998.
27. Koopman R, Manders RJ, Jonkers RA, Hul GB, Kuipers H, van Loon LJ. Intramyocellular lipid and glycogen content are reduced following resistance exercise in untrained healthy males. *Eur J Appl Physiol* 96: 525–534, 2005.
28. Koopman R, Schaart G, Hesselink MK. Optimisation of oil red O staining permits combination with immunofluorescence and automated quantification of lipids. *Histochem Cell Biol* 116: 63–68, 2001.
29. Koves TR, Noland RC, Bates AL, Henes ST, Muoio DM, Cortright RN. Subsarcolemmal and intermyofibrillar mitochondria play distinct roles in regulating skeletal muscle fatty acid metabolism. *Am J Physiol Cell Physiol* 288: C1074–C1082, 2005.
30. Krieger DA, Tate CA, McMillin-Wood J, Booth FW. Populations of rat skeletal muscle mitochondria after exercise and immobilization. *J Appl Physiol* 48: 23–28, 1980.
31. Krssak M, Petersen KF, Bergeron R, Price T, Laurent D, Rothman DL, Roden M, Shulman GI. Intramuscular glycogen and intramyocellular lipid utilization during prolonged exercise and recovery in man: a ¹³C and ¹H nuclear magnetic resonance spectroscopy study. *J Clin Endocrinol Metab* 85: 748–754, 2000.
32. Mabuchi K, Sreter FA. Actomyosin ATPase. II. Fiber typing by histochemical ATPase reaction. *Muscle Nerve* 3: 233–239, 1980.
33. Malenfant P, Tremblay A, Doucet E, Imbeault P, Simoneau JA, Joanisse DR. Elevated intramyocellular lipid concentration in obese subjects is not reduced after diet and exercise training. *Am J Physiol Endocrinol Metab* 280: E632–E639, 2001.
34. Peronnet F, Massicotte D. Table of nonprotein respiratory quotient: an update. *Can J Sport Sci* 16: 23–29, 1991.
35. Phillips SM, Green HJ, Tarnopolsky MA, Heigenhauser GJ, Grant SM. Progressive effect of endurance training on metabolic adaptations in working skeletal muscle. *Am J Physiol Endocrinol Metab* 270: E265–E272, 1996.
36. Prats C, Donsmark M, Qvortrup K, Londo C, Sztalryd C, Holm C, Galbo H, Ploug T. Decrease in intramuscular lipid droplets and translocation of HSL in response to muscle contraction and epinephrine. *J Lipid Res* 47: 2392–2399, 2006.
37. Ritov VB, Menshikova EV, He J, Ferrell RE, Goodpaster BH, Kelley DE. Deficiency of subsarcolemmal mitochondria in obesity and type 2 diabetes. *Diabetes* 54: 8–14, 2005.
38. Roepstorff C, Donsmark M, Thiele M, Vistisen B, Stewart G, Vissing K, Schjerling P, Hardie DG, Galbo H, Kiens B. Sex differences in hormone-sensitive lipase expression, activity, and phosphorylation in skeletal muscle at rest and during exercise. *Am J Physiol Endocrinol Metab* 291: E1106–E1114, 2006.
39. Roepstorff C, Steffensen CH, Madsen M, Stallknecht B, Kanstrup IL, Richter EA, Kiens B. Gender differences in substrate utilization during submaximal exercise in endurance-trained subjects. *Am J Physiol Endocrinol Metab* 282: E435–E447, 2002.
40. Romijn JA, Coyle EF, Sidossis LS, Gastaldelli A, Horowitz JF, Endert E, Wolfe RR. Regulation of endogenous fat and carbohydrate metabolism in relation to exercise intensity and duration. *Am J Physiol Endocrinol Metab* 265: E380–E391, 1993.
41. Sidossis LS, Coggan AR, Gastaldelli A, Wolfe RR. A new correction factor for use in tracer estimations of plasma fatty acid oxidation. *Am J Physiol Endocrinol Metab* 269: E649–E656, 1995.
42. Siri WE. The gross composition of the body. *Adv Biol Med Phys* 4: 239–280, 1956.
43. Starling RD, Trappe TA, Parcell AC, Kerr CG, Fink WJ, Costill DL. Effects of diet on muscle triglyceride and endurance performance. *J Appl Physiol* 82: 1185–1189, 1997.
44. Staron RS, Hikida RS, Murray TF, Hagerman FC, Hagerman MT. Lipid depletion and repletion in skeletal muscle following a marathon. *J Neurol Sci* 94: 29–40, 1989.
45. Steele R. Influences of glucose loading and of injected insulin on hepatic glucose output. *Ann NY Acad Sci* 82: 420–430, 1959.
46. Steffensen CH, Roepstorff C, Madsen M, Kiens B. Myocellular triacylglycerol breakdown in females but not in males during exercise. *Am J Physiol Endocrinol Metab* 282: E634–E642, 2002.
47. van Loon LJ. Use of intramuscular triacylglycerol as a substrate source during exercise in humans. *J Appl Physiol* 97: 1170–1187, 2004.
48. van Loon LJ, Greenhaff PL, Constantin-Teodosiu D, Saris WH, Wagenmakers AJ. The effects of increasing exercise intensity on muscle fuel utilisation in humans. *J Physiol* 536: 295–304, 2001.
49. van Loon LJ, Koopman R, Manders R, van der Weegen W, van Kranenburg GP, Keizer HA. Intramyocellular lipid content in type 2 diabetes patients compared with overweight sedentary men and highly trained endurance athletes. *Am J Physiol Endocrinol Metab* 287: E558–E565, 2004.
50. van Loon LJ, Koopman R, Schrauwen P, Stegen J, Wagenmakers AJ. The use of the [^{1,2-13}C]acetate recovery factor in metabolic research. *Eur J Appl Physiol* 89: 377–383, 2003.
51. van Loon LJ, Koopman R, Stegen JH, Wagenmakers AJ, Keizer HA, Saris WH. Intramyocellular lipids form an important substrate source during moderate intensity exercise in endurance-trained males in a fasted state. *J Physiol* 553: 611–625, 2003.
52. van Loon LJ, Schrauwen-Hinderling VB, Koopman R, Wagenmakers AJ, Hesselink MK, Schaart G, Kooi ME, Saris WH. Influence of prolonged endurance cycling and recovery diet on intramuscular triglyceride content in trained males. *Am J Physiol Endocrinol Metab* 285: E804–E811, 2003.
53. Watt MJ, Heigenhauser GJ, Dyck DJ, Spriet LL. Intramuscular triacylglycerol, glycogen and acetyl group metabolism during 4 h of moderate exercise in man. *J Physiol* 541: 969–978, 2002.
54. Watt MJ, Heigenhauser GJ, Spriet LL. Intramuscular triacylglycerol utilization in human skeletal muscle during exercise: is there a controversy? *J Appl Physiol* 93: 1185–1195, 2002.
55. Wendling PS, Peters SJ, Heigenhauser GJ, Spriet LL. Variability of triacylglycerol content in human skeletal muscle biopsy samples. *J Appl Physiol* 81: 1150–1155, 1996.
56. White LJ, Ferguson MA, McCoy SC, Kim H. Intramyocellular lipid changes in men and women during aerobic exercise: a (¹H)-magnetic resonance spectroscopy study. *J Clin Endocrinol Metab* 88: 5638–5643, 2003.
57. Wolfe RR, Jahoor F. Recovery of labeled CO₂ during the infusion of C-1- vs C-2-labeled acetate: implications for tracer studies of substrate oxidation. *Am J Clin Nutr* 51: 248–252, 1990.
58. Zehnder M, Christ ER, Ith M, Acheson KJ, Pouteau E, Kreis R, Trepp R, Diem P, Boesch C, Decombaz J. Intramyocellular lipid stores increase markedly in athletes after 1.5 days lipid supplementation and are utilized during exercise in proportion to their content. *Eur J Appl Physiol*, 98: 341–354, 2006.
59. Zehnder M, Ith M, Kreis R, Saris W, Boutellier U, Boesch C. Gender-specific usage of intramyocellular lipids and glycogen during exercise. *Med Sci Sports Exerc* 37: 1517–1524, 2005.